Am J Physiol Endocrinol Metab 313: E48–E62, 2017.
First published March 21, 2017; doi:10.1152/ajpendo.00304.2016.

RESEARCH ARTICLE

Effects of genetic deletion of soluble 5′-nucleotidases NT5C1A and NT5C2 on AMPK activation and nucleotide levels in contracting mouse skeletal muscles

Samanta Kviklyte,[1] Didier Vertommen,[1] Xavier Yerna,[2] Harriet Andersén,[3] Xiufeng Xu,[3] Philippe Gailly,[2] Mohammad Bohlooly-Y,[3] Jan Oscarsson,[3] and Mark H. Rider[1]

[1]*de Duve Institute, Université catholique de Louvain, Brussels, Belgium;* [2]*Institute of Neuroscience, Université catholique de Louvain, Brussels, Belgium; and* [3]*AstraZeneca Research and Development, Mölndal, Sweden*

Submitted 3 August 2016; accepted in final form 13 March 2017

Kviklyte S, Vertommen D, Yerna X, Andersén H, Xu X, Gailly P, Bohlooly-Y M, Oscarsson J, Rider MH. Effects of genetic deletion of soluble 5′-nucleotidases NT5C1A and NT5C2 on AMPK activation and nucleotide levels in contracting mouse skeletal muscles. *Am J Physiol Endocrinol Metab* 313: E48–E62, 2017. First published March 21, 2017; doi:10.1152/ajpendo.00304.2016.—AMP-activated protein kinase (AMPK) plays a key role in energy homeostasis and is activated in response to contraction-induced ATP depletion in skeletal muscle via a rise in intracellular AMP/ADP concentrations. AMP can be deaminated by AMP-deaminase (AMPD) to IMP, which is hydrolyzed to inosine by cytosolic 5′-nucleotidase II (NT5C2). AMP can also be hydrolyzed to adenosine by cytosolic 5′-nucleotidase 1A (NT5C1A). Previous gene silencing and overexpression studies indicated control of AMPK activation by NT5C enzymes. In the present study using gene knockout mouse models, we investigated the effects of NT5C1A and NT5C2 deletion on intracellular adenine nucleotide levels and AMPK activation in electrically stimulated skeletal muscles. Surprisingly, NT5C enzyme knockout did not lead to enhanced AMP or ADP concentrations in response to contraction, with no potentiation of increases in AMPK activity in extensor digitorum longus (EDL) and soleus mouse muscles. Moreover, dual blockade of AMP metabolism in EDL using an AMPD inhibitor combined with NT5C1A deletion did not enhance rises in AMP and ADP or increased AMPK activation by electrical stimulation. The results on muscles from the NT5C knockout mice contradict previous findings where AMP levels and AMPK activity were shown to be modulated by NT5C enzymes.

AMPK; NT5C1A; NT5C2; muscle; contraction

A MAJOR DEFECT IN TYPE 2 DIABETES (T2D) is an impairment of tissue sensitivity to insulin. In the absorptive state, muscle glucose uptake accounts for ~75% of total glucose uptake by tissues and organs of the body, and in individuals with T2D, the major impairment of insulin-mediated glucose uptake can be attributed to a defect in skeletal muscle (6). Pharmaceutical strategies to enhance skeletal muscle glucose uptake would thus be beneficial for counteracting the symptoms of T2D. AMPK is an energy-sensing protein kinase that has emerged as a potential drug target for the treatment of T2D and other metabolic disorders (8, 24). Muscle contraction causes ATP depletion leading to a rise in ADP and AMP, the latter being responsible for allosterically stimulating AMPK activity. AMP and ADP also activate AMPK by preventing dephosphorylation of the α-subunit Thr^{172} activation loop residue targeted by upstream kinases, and AMP promotes AMPKα Thr^{172} phosphorylation by the upstream liver kinase B1 (LKB1) (8). Once activated, AMPK switches on ATP-generating processes while simultaneously switching off energy consuming pathways such as lipogenesis via phosphorylation of its best substrate, acetyl-CoA carboxylase (ACC). AMPK activation in muscle during contraction also stimulates glucose uptake, independent of insulin, which partly underlies the beneficial effects of exercise for the management of T2D (21). The contraction-induced stimulation of glucose uptake as a result of AMPK activation is due to increased GLUT4 translocation to the plasma membrane, which involves TBC1D1 and FYVE domain-containing phosphatidylinositol 3-phosphate 5-kinase phosphorylation, both of which have been proposed as mediators (15, 21, 22).

AMPK exists as heterotrimers comprising a catalytic α-subunit (α_1 or α_2) associated with two regulatory β (β_1 or β_2) and γ (γ_1, γ_2, or γ_3) subunits encoded by separate genes (8). The γ-subunit possesses four tandem cystathionine β-synthase (CBS) repeats, potentially providing four sites for nucleotide binding, but one site is empty and another contains permanently bound AMP (26). To date, there have been no pharmacological drugs used to treat T2D that directly activate AMPK. Metformin, the most prescribed oral antidiabetic drug, acts mainly on the liver to decrease hepatic glucose production, but whether AMPK is involved is controversial (7). Metformin activates AMPK indirectly by inhibiting the mitochondrial respiratory chain and increasing intracellular AMP:ATP and ADP:ATP ratios. Compounds A769662 (5) and 991 (12, 27), on the other hand, are direct AMPK activators, which, like AMP, inhibit AMPKα Thr^{172} dephosphorylation, but not by binding to the AMPK γ-subunits. Structural studies showed that compound 991 binds in a cleft between the small lobe of the AMPKα-subunit kinase domain and the AMPKβ-subunit carbohydrate-binding module (27), which is also the binding site for A769662l, and is termed the allosteric drug and metabolite binding site (ADaM) (14). Compound 991 is much more potent (5- to 10-fold) than A769662 (27) and has been shown to stimulate AMPK activity of both AMPKβ_1- and

Address for reprint requests and other correspondence: M. H. Rider, de Duve Institute-UCL, Avenue Hippocrate 75, bte B1.74.02, B-1200 Brussels, Belgium (e-mail: mark.rider@uclouvain.be).

AMPKβ_2-containing complexes and to increase glucose transport in isolated mouse skeletal muscle in vitro (12).

The intracellular concentration of AMP depends on its binding to intracellular proteins and on the activities of adenylate kinase, AMP deaminase (AMPD), 5′-nucleotidases (NT5Cs), adenosine kinase, and other salvage pathway enzymes (Fig. 1). AMPD1 is highly expressed in skeletal muscle, AMPD2 is predominant in nonmuscle tissues, and AMPD3 is found in erythrocytes (16–18). There are seven human NT5Cs, of which cytosolic NT5C1A is specific for AMP and is expressed in muscle and heart, whereas cytosolic NT5C2 preferentially hydrolyzes IMP and is ubiquitous (2). Because of their high catalytic efficiency, despite their high K_Ms for nucleotides, these enzymes could influence intracellular AMP concentrations. Overexpression of AMP-metabolizing enzymes in HEK293 cells indicated that whereas AMPD seemed to have little control over intracellular AMP concentrations, NT5C1A exerted a large proportion of control over AMP, and its overexpression reduced the oligomycin-induced increases in AMP and ADP and reduced AMPK activation (20). Pharmacological AMPD inhibition potentiated AMPK activation by contraction in incubated rat skeletal muscles without increasing glucose uptake, whereas genetic AMPD1 deletion resulted in higher AMP levels during contraction of incubated mouse muscles, but AMPK activation was moderate and was observed only in soleus muscle (19). Also, administration of inhibitors did not improve glucose control in insulin-resistant or diabetic rodent disease models (1). On the other hand, gene silencing of NT5C2 in human myotubes and silencing of NT5C1A in mouse muscle resulted in an increased intracellular AMP:ATP ratio, increased AMPKα Thr^{172} phosphorylation, and increased AMPK downstream signaling (11). The aim of the present study was to determine whether AMPK activation in muscles from mice bearing whole body deletions of NT5C1A and NT5C2 could be potentiated by contraction to support drug targeting these enzymes as a strategy for the treatment of T2D.

MATERIALS AND METHODS

Materials. Protease inhibitor cocktail tablets (Roche Diagnostics) and Protein G Sepharose (GE Healthcare) were from the indicated sources. Anti-total AMPKα_1 and anti-total AMPKα_2 antibodies were provided by Prof. Grahame Hardie (University of Dundee, UK). Anti-total AMPKγ_1 and anti-total AMPKγ_3 antibodies were generated as described (4) and kindly provided by Kei Sakamoto (Nestle, Switzerland). Anti-pACC (catalog number 07-303, raised against rat ACC1 but recognizing Ser^{212} in mouse ACC2) and anti-total ACC (05-1098) antibodies were from Millipore. Anti-total eukaryotic elongation factor-2 (eEF2) (sc-13003) was from Santa Cruz Biotechnology. Anti-pThr^{172} AMPKα (2535) and anti-p$Ser^{485/491}$ AMPK$\alpha_1\alpha_2$ (4185) antibodies were from Cell Signaling. Anti-total AMPKβ_1 (AF2854) and anti-total AMPKβ_2 (MAB3808) were from R&D systems. AMARA AMPK substrate peptide (AMARAASAAALRRR) was synthesized by V. Stroobant (Ludwig Institute for Cancer Research, Brussels, Belgium). Whatman phosphocellulose P81 paper sheets, [γ-^{32}P] ATP, D-[1-^{14}C] mannitol, and 2-deoxy-D-[1-^{3}H] glucose were from PerkinElmer. Solvents and acids for HPLC analysis were from Biosolve. All other chemicals were from Sigma-Aldrich.

Generation of NT5C1A- and NT5C2-deficient mice. All experiments were approved by the Gothenburg Ethics Committee for Experimental Animals. NT5C1A- and NT5C2-deficient mice were generated on pure C57Bl/6 strain genetic background mice. A targeting vector for homologous recombination in the mouse was prepared from a C57 BAC clone (ResGen, Invitrogen). DNA fragments of 5.7, 5.1, and 1.5 kb for NT5C1A and fragments of 6, 2.1, and 2 kb for NT5C2 were extracted and (for 5′ deletion and 3′ homology regions, respectively) cloned into a modified loxP floxed plasmid. The deletion fragment includes exons 2, 3, and 4 of the NT5C1A gene (Fig. 2*A*) and exon 3 of the NT5C2 gene (Fig. 2*B*). To select for positively targeted embryonic stem (ES) cells, a floxed neomycin phosphotransferase (Neo) selectable marker cassette was also included in the targeting vector. The targeting vectors were linearized and electroporated into C57BL6 (Prx) mouse ES cells. Neo-resistant clones were analyzed for correct integration by PCR and confirmed by Southern blotting (data not shown). One clone was expanded and injected into Balb/cAnNCrl blastocysts to generate chimeric mice. Chimeric males were bred to C57BL6 females to produce agouti heterozygous mice. For generation of NT5C1A- and NT5C2-null mice, heterozygous F_1 males were bred to Rosa26Cre transgenic mice (C57BL6 background) to delete the loxP floxed region including the desired exons and Neo cassette. NT5C1A and NT5C2 wild-type and null mice were obtained from intercross mating heterozygous animals housed under a 12:12-h light-dark cycle. Offspring were genotyped at weaning by PCR using specific primers to detect the wild-type and null alleles in genomic DNA isolated from tail tip biopsies. NT5C1A forward primer sequences were 5′-CAAAGGACTTCTTGTTCCGTA and 5′-GCCAGTGCTAAGGTGAGATTA (285- and 395-bp fragments), and the reverse primer sequence was 5′-AAGGGTTTGATGTGTCTAGGG for both wild-type and knockout mice. The NT5C2 forward primer sequence was 5′-GGAGATTCTACCATTTGCAACC and reverse primer sequences were 5′-CCCTCCCTTGCCTTTCTAAT and 5′-GACTCACCCGGTCTCAAAAA (238- and 208-bp fragments) for both wild-type and knockout mice.

Expression of NT5C1A and NT5C2 mRNA in mouse tissues. Total mRNA was extracted from mouse tissues using 1 ml of TRIzol reagent (Life Technologies) per 100 mg of tissue according to the manufacturer's instructions. RNA was quantified by Nanodrop, and 500 ng was used for cDNA synthesis using the Moloney murine leukemia virus RT kit (Life Technologies) according to the manufacturer's protocol. Reverse transcription products were diluted 1:3 in nuclease-free water, and 1 μl was used for quantitative PCR (qPCR) with the Kapa Sybr Fast qPCR kit (Kapa Biosystems) in a CFX96 real-time PCR thermocycler (Bio-Rad). The program was 40 cycles at 95°C for 10 s, 62–66°C for 10 s, 72°C for 30 s, and a final melting curve. PCR reactions were carried out in a final volume of 10 μl with 1 μM of each of the primers for mouse NT5C1A (CTCAG-

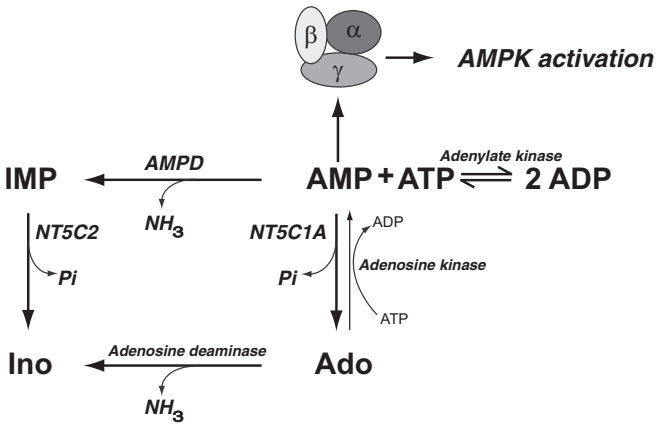

Fig. 1. Scheme showing the pathways of purine nucleotide metabolism via AMP deaminase (AMPD), NT5C1A, NT5C2, and other enzymes. Enzymes are indicated in italics. Ino, inosine; Ado, adenosine.

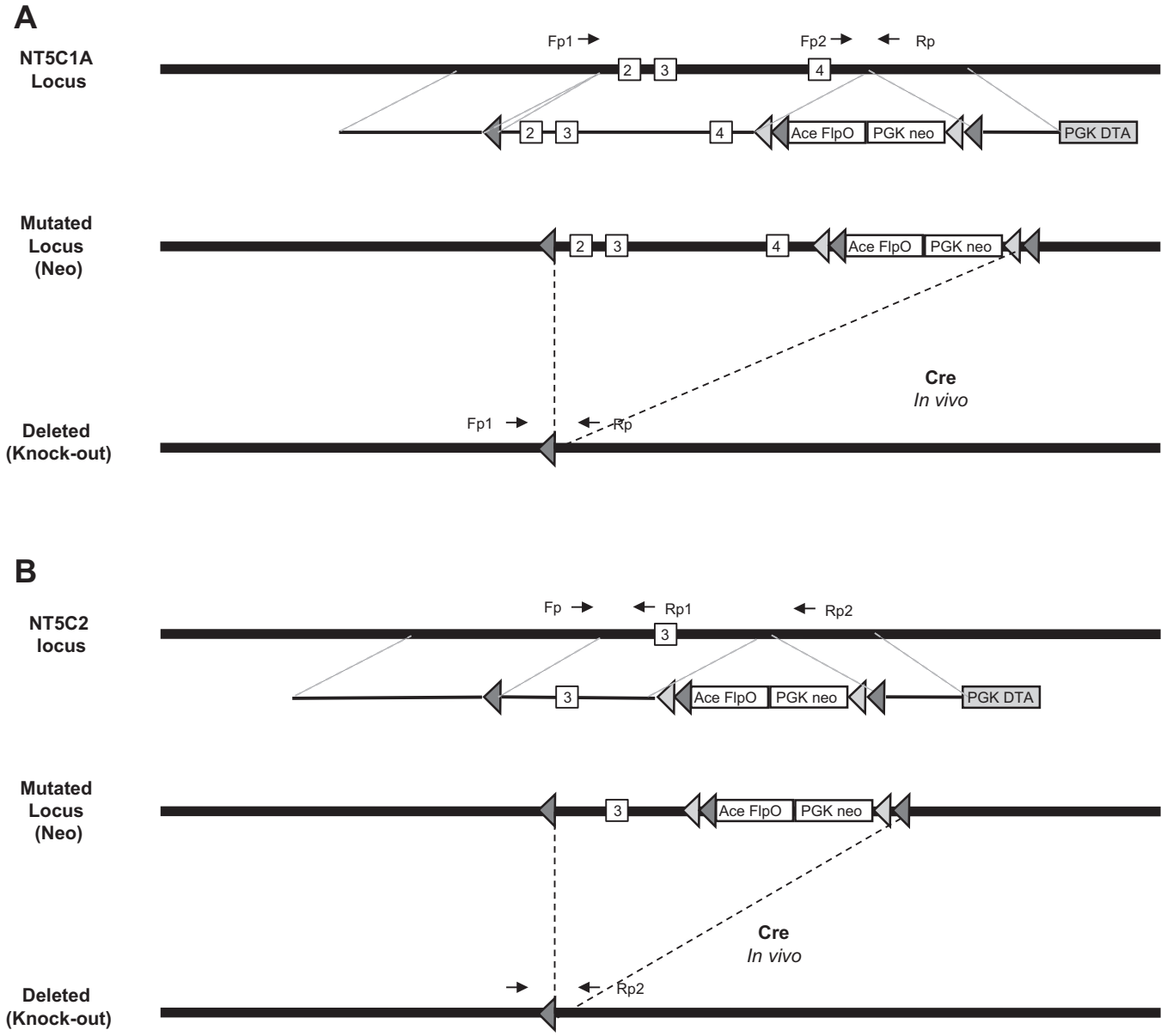

Fig. 2. Generation of the NT5C1A and NT5C2 mouse lines. The scheme shows the NT5C1A (*A*) and NT5C2 (*B*) genes and targeting vectors.

GTGGGAGTTCGTCTCA, GGTAGCAGATGGGGCTATTCC) and NT5C2 (TGACCGCTTACAGAATGCAG, CGGCTAGGGTATAATCCATATCA). NT5C2 qPCR primers were designed with Primer3 (https://biotools.umassmed.edu/bioapps/primer3_www.cgi), and NT5C1A primers were taken from PrimerBank (http://pga.mgh.harvard.edu/primerbank/index.html).

Isolated skeletal muscle incubations. All animal experiments were approved by the Animal Ethics Committee of the Université Catholique de Louvain Medical Faculty. Extensor digitorum longus (EDL) and soleus muscles were dissected from anesthetized 12- to 16-wk-old wild-type and NT5C-knockout male mice. Muscle incubations were performed as previously described (19). Briefly, skeletal muscles were continuously gassed with 95% O_2:5% CO_2 and incubated in 3 ml of Krebs-Henseleit bicarbonate buffer containing 5.5 mM glucose, 2 mM sodium pyruvate, and 0.1% (wt/vol) BSA at pH 7.4 and 30°C. Contraction was induced by electrical stimulation (100 ms for EDL and 300 ms for soleus delivered every 2 s at 100 Hz for the indicated times). After incubation, the muscles were frozen in liquid nitrogen. In experiments with AMPD inhibitor, EDL muscles were preincubated for 60 min with 27 μM compound 4 (19) or 0.1% (vol/vol) DMSO as a vehicle control, then transferred to a fresh buffer and electrically stimulated with 200-ms trains delivered every 2 s at 100 Hz for the indicated times (12) or incubated at rest for 15 min. After incubation, the muscles were frozen in liquid nitrogen.

Treadmill running experiments. Mice were placed on a treadmill for 5 min (5 m/min) and running speed was a progressively increased (1 m/min) every minute to 17 m/min, and the test was terminated after 60 min (28).

Purine nucleotide measurements. Lyophilized muscles were weighed and then extracted with 500 μl of ice-cold 0.1 M $HClO_4$/40% (vol/vol) CH_3OH (KONTES DUALL 21 all glass tissue grinder) followed by centrifugation (Eppendorf microfuge, full speed ×15 min at 4°C). Supernatants were neutralized with 1.1 M $(NH_4)_2HPO_4$, dried, and resuspended in HPLC-grade water for storage at −20°C before analysis as described (19). Nucleotide concentrations are expressed per milligram of dry weight of muscle, and the adenylate energy charge (AEC) was calculated as AEC = ([ATP]+ ½[ADP])/([ATP] + [ADP] + [AMP]).

Preparation of muscle extracts. EDL and soleus muscles were homogenized (Ultra-Turrax fitted with a T 10 disperser, 3 × 10 s) in 500 μl of ice-cold lysis buffer containing 50 mM Hepes pH 7.6, 0.1% (wt/vol) Triton X-100, 50 mM KF, 50 mM KCl, 5 mM $Na_4P_2O_7$, 1 mM EDTA, 1 mM EGTA, 5 mM sodium β-glycerolphosphate, 1 mM $NaVO_3$, and protease inhibitor cocktail. After addition of 1 mM dithiothreitol, the homogenates were rotated on a wheel for 1 h at 4°C and centrifuged (Eppendorf microfuge, full speed ×15 min at 4°C). Supernatants were taken for AMPK assay (19), immunoblotting, and protein estimation (3) using BSA as a standard. For AMPK assay, lysates were immunoprecipitated with anti-AMPKα_1 or anti-AMPKα_2 antibodies or with anti-AMPKα_1 plus anti-AMPKα_2 antibodies for total AMPK activity (19). For AMPK subunit expression analysis, extracts were prepared from EDL incubated at rest and immunoprecipitated with anti-AMPKβ_1 plus anti-AMPKβ_2 antibodies as described for immunoprecipitation with anti-AMPKα subunit antibodies (19). Proteins in the immunoprecipitate and supernatant were separated by SDS-PAGE for immunoblotting with specific anti-AMPK subunit antibodies.

Glucose uptake in incubated skeletal muscles. Radioactivity incorporated in 2-deoxyglucose-6-phosphate was measured in EDL mouse muscles after incubation in 3 ml of Krebs-Henseleit buffer containing 2-deoxy-D-[1-^{3}H]glucose (0.25 μCi/mmol) and D-[1-^{14}C] mannitol (0.1 μCi/ml) at 30°C for 20 min (13).

Statistical analysis. Results are expressed as means ± SE. Statistical analysis was performed using a Student's unpaired two-sided *t*-test, by one-way ANOVA, or by two-way ANOVA with an appropriate post hoc test. $P < 0.05$ was considered significant.

RESULTS

Quantification of NT5C1A and NT5C2 expression in tissues from wild-type vs. knockout mice. NT5C1A- and NT5C2-knockout mice had similar body weights compared with their wild-type littermates and displayed no obvious phenotype (data not shown). Commercial NT5C1A and NT5C2 antibodies we tested did not give clean enough signals to assess expression of the proteins by immunoblotting tissue extracts. Therefore, we resorted to tissue mRNA extraction and expression analysis by quantitative RT-PCR. Human mRNA profiling suggests predominant NT5C1A expression in skeletal muscle (see Bio GPS, http://biogps.org/#goto=genereport&id=84618) as confirmed (10, 23). Abundant expression was also reported in mouse tibialis anterior (TA), but NT5C1A mRNA was undetectable in primary human myotubes (11). Here, we found that NT5C1A mRNA was expressed in TA, heart, and liver from wild-type mice (Fig. 3). TA muscle was analyzed rather than EDL (mainly type II fibers) and soleus (mainly type I fibers) muscles to obtain sufficient material for mRNA extraction, and it contains a mixture of type I and II fibers. In tissues from NT5C1A-knockout mice, NT5C1A mRNA expression was very low or undetectable in TA, heart, and liver (Fig. 3). NT5C2 expression is ubiquitous in humans (Bio GPS http://biogps.org/#goto=genereport&id=76952) and expressed in all organs and tissues of vertebrates (25). NT5C2 mRNA was expressed in TA, heart, and liver with expression being highest in heart (Fig. 4). In tissues from NT5C2-deleted mice, NT5C2 mRNA expression was undetectable in TA, heart, and liver (Fig. 4). Deletion of either NT5C1A or NT5C2 enzyme did not result in compensatory changes in mRNA levels of other NT5C enzymes or AMPD1 in TA muscle (Fig. 3, *D* and *E* and Fig. 4, *D* and *E*).

Contraction-induced changes in AMPK activity, glucose uptake, and purine nucleotide levels in skeletal muscles from wild-type vs. NT5C2-knockout mice. Electrical stimulation led to an approximately fourfold increase in AMPK activity in wild-type EDL muscles compared with the resting condition, but contraction-induced AMPK activation in EDL muscles from NT5C2-knockout mice did not differ from that observed in EDL from wild-type mice (Fig. 5*A*). Also, the increase in AMPK activity induced by electrical stimulation

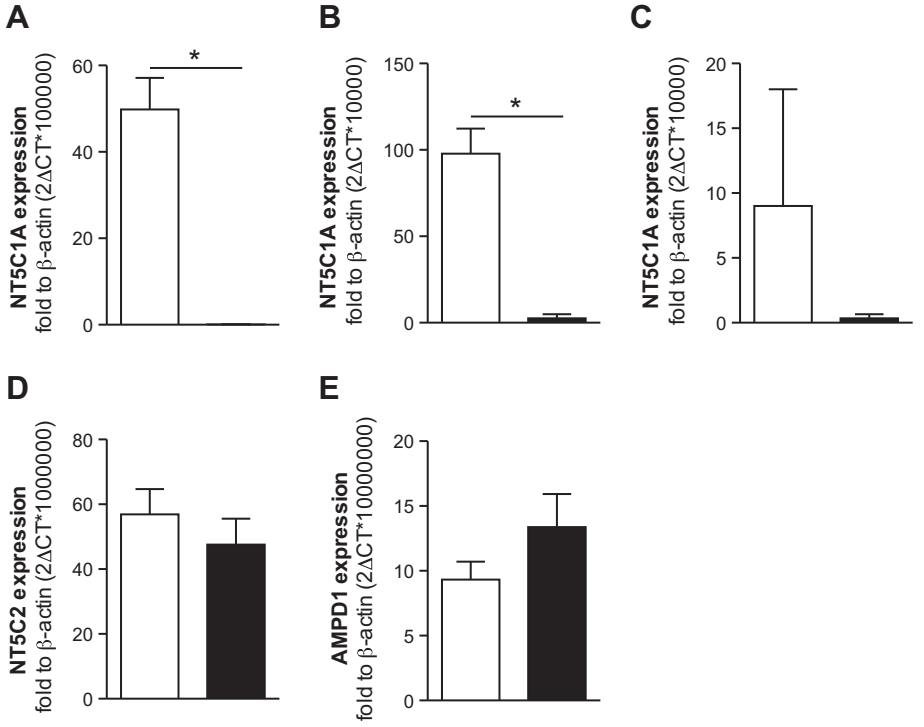

Fig. 3. Messenger RNA expression analysis of tissues from wild-type vs. NT5C1A-knockout mice. NT5C1A expression in tibialis anterior (TA) muscle (*A*), heart (*B*), and liver (*C*) along with NT5C2 (*D*) and AMPD1 (*E*) expression in TA muscle from wild-type (open bars) vs. NT5C1A-knockout mice (black bars). Values are means ± SE of four separate determinations. *Significant difference, $P < 0.05$.

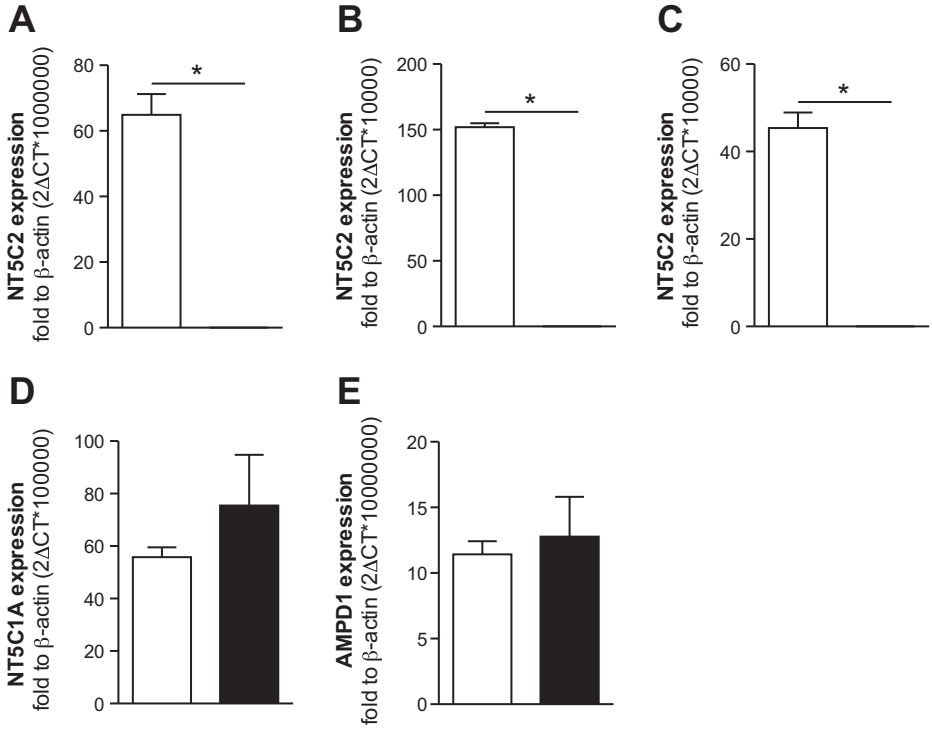

Fig. 4. Messenger RNA expression analysis of tissues from wild-type vs. NT5C2-knockout mice. NT5C2 expression in TA muscle (*A*), heart (*B*), and liver (*C*) along with NT5C1A (*D*) and AMPD1 (*E*) expression in TA muscle from wild-type (open bars) vs. NT5C2-knockout mice (black bars). Values are means ± SE of four separate determinations. *Significant difference, $P < 0.05$.

was the same in incubated soleus muscles from wild-type vs. NT5C2-knockout mice (Fig. 5*B*). Increases in total AMPK activity (AMPKα_1 + AMPKα_2) in response to contraction observed in EDL and soleus muscles from wild-type vs. NT5C2-knockout mice were similar to the increases in AMPK activity of AMPKα_1- and AMPKα_2-containing complexes observed after immunoprecipitation with anti-AMPKα_1 or anti-AMPKα_2 antibodies (data not shown). Electrical stimulation of EDL from wild-type mice led to an ~50% increase in glucose uptake, which was increased to the same extent by contraction in EDL from NT5C2-knockout mice (Fig. 5*C*). Similar rates of glucose uptake were reached in contracting soleus muscles from wild-type and NT5C2-knockout mice, although basal glucose uptake was somewhat less in soleus from NT5C2-knockout mice compared with wild-type mice (Fig. 5*D*). The lack of effect of NT5C2 deletion on contraction-induced increases in glucose uptake is consistent with the fact that AMPK activation induced by contraction was unaffected by NT5C2 deletion in both muscle types (Fig. 5, *A* and *B*). Moreover, increases in AMPKα pThr^{172} and downstream ACC pSer^{212} phosphorylation induced by electrical stimulation of EDL (Fig. 5*E*) and soleus (Fig. 5*F*) muscles from wild-type and NT5C2-knockout mice were similar.

Nucleotide levels were measured by HPLC in muscles that had been freeze-stopped in liquid N_2 and extracted in perchloric acid. Nucleotide concentrations were expressed as nmol/mg of muscle dry weight with values comparable to those observed in electrically stimulated rat epitrochlearis muscles (12). Electrical stimulation significantly decreased ATP levels only in EDL from wild-type mice (Fig. 6*A*) with no significant rise in ADP either in EDL muscles from wild-type or NT5C2-knockout mice (Fig. 6*B*). Similar increases of approximately threefold in AMP levels were observed in EDL from wild-type and NT5C2-knockout mice after electrical stimulation (Fig. 6*C*). NT5C2-knockout resulted in potentiation (~40%) of the rise in IMP concentrations observed during electrical stimulation in EDL (Fig. 6*D*), which is consistent with significant AMPD flux during contraction (19) and deletion of the nucleotidase. There were no significant differences in the contraction-induced increases in adenosine and inosine in EDL from NT5C2-knockout mice compared with wild-type mice or in the increase in inosine levels at rest as a result of NT5C2 deletion (Figs. 6, *E* and *F*). In EDL from wild-type vs. NT5C2-knockout mice, an increase of approximately fourfold and 50% in AMP:ATP (Fig. 6*G*) and ADP:ATP (Fig. 6*H*) ratios, respectively, following contraction were comparable, and there was a similar slight drop in AEC in EDL from both wild-type and NT5C2-knockout mice after electrical stimulation (Fig. 6*I*).

On the whole, changes in purine nucleotide concentrations observed after electrical stimulation of soleus muscles from wild-type vs. NT5C2-knockout mice (Fig. 7) were similar to those observed in EDL muscle (Fig. 6), except that the contraction-induced enhancement of IMP levels due to NT5C2 deletion was not significant (Fig. 7*D*). Also, electrical stimulation did not significantly increase the AMP:ATP and ADP:ATP ratios or significantly decrease the AEC in EDL from wild-type or NT5C2-knockout mice (Fig. 7, *G–I*).

Contraction-induced changes in AMPK activity, glucose uptake, and purine nucleotide levels in skeletal muscles from wild-type vs. NT5C1A-knockout mice. Deletion of NT5C1A in skeletal muscle was expected to enhance AMPK activation during contraction because NT5C1A directly hydrolyzes AMP (Fig. 1). In EDL from wild-type mice subjected to 15 min of electrical stimulation, AMPK activity of immunoprecipitated AMPKα_1- and AMPKα_2-containing complexes increased fourfold to fivefold, respectively (Fig. 8, *A* and *C*). Surprisingly, contraction-induced AMPK activation of AMPKα_2-containing complexes was significantly decreased in EDL from

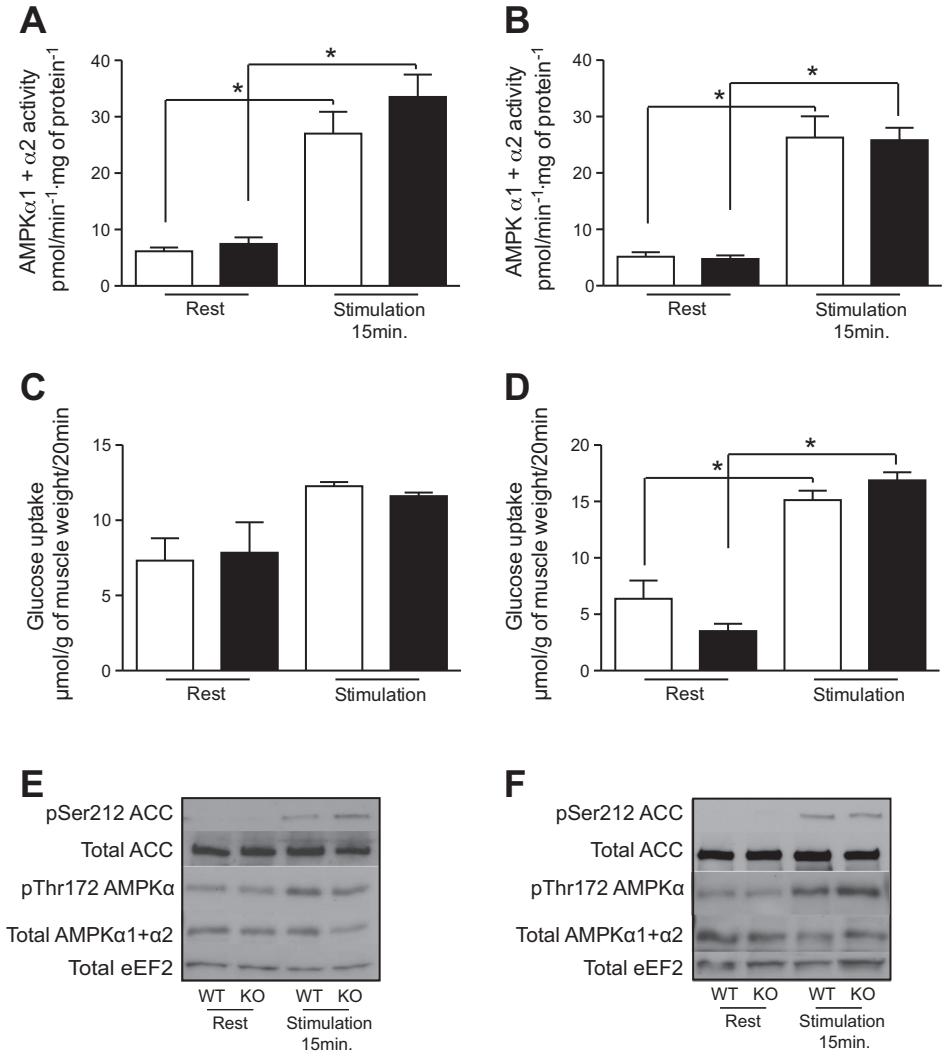

Fig. 5. AMP-activated protein kinase (AMPK) activities, glucose uptake, and acetyl-CoA carboxylase (ACC) phosphorylation in skeletal muscles from wild-type vs. NT5C2-knockout mice incubated with and without electrical stimulation. Extensor digitorum longus (EDL) (*A*) and soleus (*B*) muscles from wild-type (open bars) and NT5C2-knockout (black bars) mice were incubated without electrical stimulation (Rest) or subjected to electrical stimulation for 15 min as described in MATERIALS AND METHODS. Extracts were immunoprecipitated with anti-AMPKα_1 plus anti-AMPKα_2 antibodies before AMPK assay. Values are means ± SE of five separate experiments. Glucose uptake was measured in electrically stimulated or resting EDL (*C*) and soleus (*D*) muscles by incubation for 20 min with 2-deoxy-D-[1-^{3}H] glucose (0.25 μCi/ml) and D-[1-^{14}C] mannitol (0.1 μCi/ml). Values are means ± SE of four separate experiments and the data were analyzed by one-way ANOVA. *Significant difference, $P < 0.05$. EDL (*E*) and soleus (*F*) extracts from wild-type and NT5C2-knockout mice were also immunoblotted with the indicated antibodies and representative blots are shown from at least two separate experiments.

NT5C1A-knockout mice compared with wild-type mice (Fig. 8*C*). Although AMPK activation of AMPKα_1- and AMPKα_2-containing complexes observed following electrical stimulation of soleus (Fig. 8, *B* and *D*) from wild-type mice was somewhat less than that observed in EDL (Fig. 8, *A* and *C*), there was nevertheless a significant decrease in AMPK activation of AMPKα_2-containing complexes in soleus from NT5C1A-knockout vs. wild-type mice in response to contraction (Fig. 8*D*). After shorter times of electrical stimulation of 5 min, total AMPK activation of AMPKα_1- plus AMPKα_2-containing complexes was unchanged in EDL or soleus from wild-type vs. NT5C1A-knockout mice (Fig. 8, *E* and *F*). NT5C1A deletion had no effect on the approximately twofold and fourfold increases in glucose uptake observed after electrical stimulation of EDL and soleus muscles, respectively, from wild-type mice (Fig. 8, *G* and *H*). Finally, no differences were observed when wild-type and NT5C1A-knockout mice were subjected to treadmill exercise endurance (data not shown).

Electrical stimulation of EDL from NT5C1A-knockout vs. wild-type mice led to similar significant decreases in intracellular ATP content, whereas increases in ADP and AMP observed during contraction were only significant in EDL from wild-type mice (Fig. 9, *A–C*). Contraction significantly increased IMP levels only in EDL from NT5C1A-knockout mice (Fig. 9*D*). However, the increase in adenosine observed after contraction in EDL from wild-type mice was markedly reduced in contracting EDL from NT5C1A-knockout mice, consistent with deletion of the nucleotidase (Fig. 9*E*). Also, the rise in inosine observed after electrical stimulation in EDL from wild-type mice was also significantly decreased in EDL from NT5C1A-knockout mice (Fig. 9*F*). Electrical stimulation did not significantly increase the AMP:ATP or ADP:ATP ratios in EDL from wild-type or NT5C1A-knockout mice (Fig. 9, *G* and *H*). The fall in AEC observed after electrical stimulation was similar in EDL from wild-type and NT5C1A-knockout mice (Fig. 9*I*).

Electrical stimulation of soleus from NT5C1A-knockout mice led to a significant drop in intracellular ATP, but there was no significant increase in ADP levels in soleus either from wild-type or NT5C1A-knockout mice (Fig. 10, *A* and *B*). Contraction resulted in significantly increased AMP and IMP levels only in soleus muscle from NT5C1A-knockout mice, and there was no significant enhancement vs. wild-type mice (Fig. 10, *C* and *D*). However, the increase in adenosine observed after contraction in soleus muscle from wild-type mice

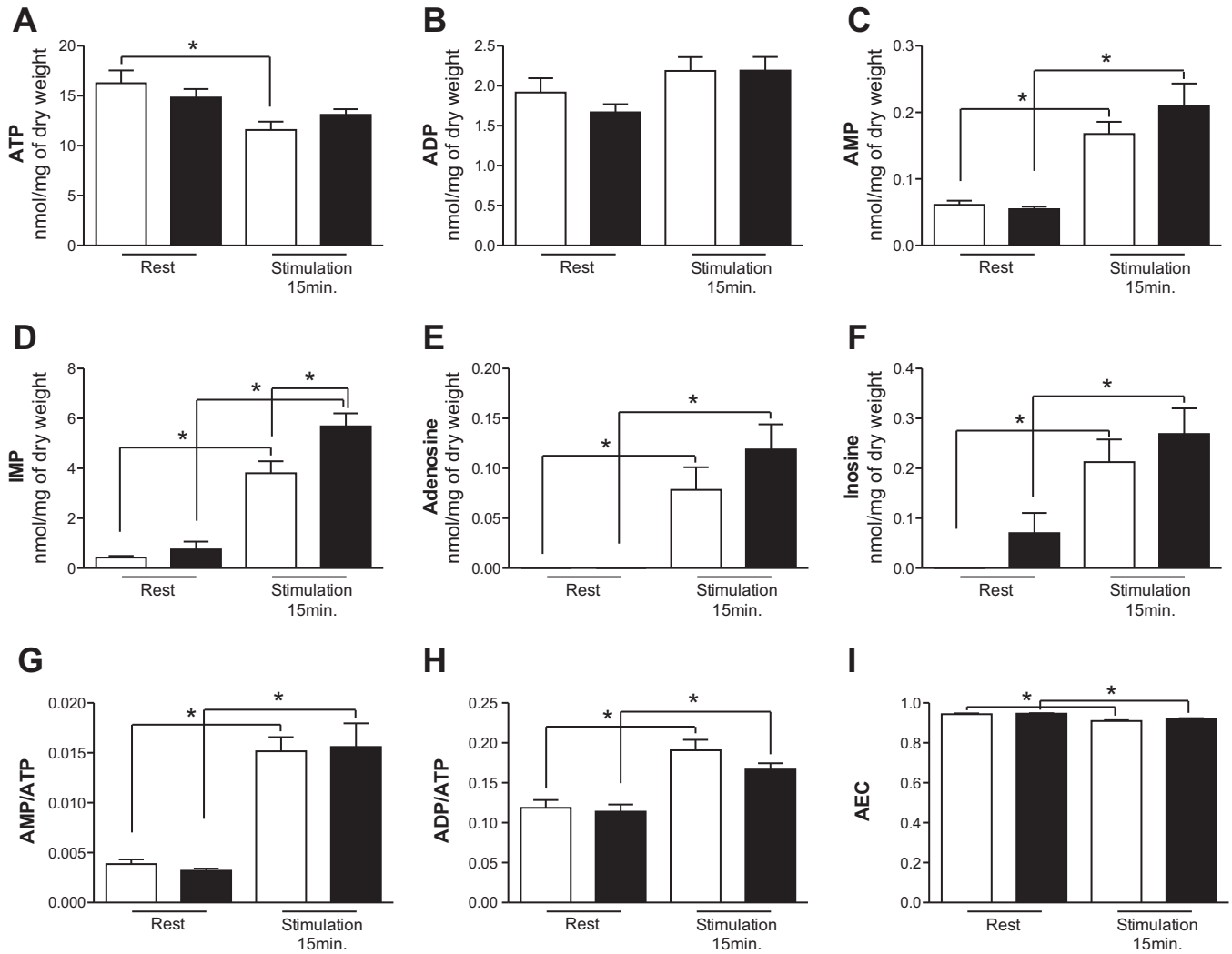

Fig. 6. Purine nucleotide levels in EDL muscles from wild-type vs. NT5C2-knockout mice incubated with and without electrical stimulation. EDL muscles from wild-type (open bars) and NT5C2-knockout (black bars) mice were incubated without electrical stimulation (Rest) or subjected to electrical stimulation for 15 min as described in MATERIALS AND METHODS. Total purine nucleotide concentrations were measured in perchlorate extracts by HPLC and expressed as nmol/mg of muscle dry weight (*A–F*) for calculations of AMP:ATP ratio (*G*), ADP:ATP ratio (*H*), and adenylate energy charge (AEC) (*I*). The results are means ± SE of five separate experiments and the data were analyzed by one-way ANOVA. *Significant difference, $P < 0.05$.

was reduced to basal levels in contracting soleus from NT5C1A-knockout mice, which is consistent with deletion of the nucleotidase (Fig. 10*E*). The rise in inosine induced by contraction was not significantly different in soleus muscle from wild-type vs. NT5C1A-knockout mice (Fig. 10*F*). Contraction did not significantly increase AMP:ATP or ADP:ATP ratios in soleus from either wild-type or NT5C1A-knockout mice (Fig. 10, *G* and *H*). A significant fall in AEC after electrical stimulation was observed only in soleus muscle from NT5C1A-knockout mice (Fig. 10I).

Effects of combined AMPD pharmacological inhibition and NT5C1A-knockout on purine nucleotide levels and AMPK activation. We next tested whether dual blockade of AMP metabolism using the AMPD inhibitor compound 4 (1, 19) along with NT5C1A deletion would lead to enhanced changes in nucleotide concentrations in response to electrical stimulation. EDL muscle was chosen over soleus due to larger increases in IMP levels induced by contraction, indicative of flux through AMPD1. The drop in ATP levels following electrical stimulation was significant only in EDL muscle from NT5C1A-knockout mice incubated with or without the AMPD inhibitor compound 4 (Fig. 11*A*). Electrical stimulation did not significantly increase AMP levels in EDL from either wild-type or NT5C1A-knockout mice and there was no significant enhancement due to NT5C1A deletion by contraction either with or without compound 4 treatment (Fig. 11*C*). Although contraction did not significantly increase the AMP:ATP or ADP:ATP ratios in EDL from either wild-type or NT5C1A-knockout mice treated with or without compound 4 (Fig. 11, *G* and *H*), there was a significant enhancement of the AMP:ATP ratio due to NT5C1A deletion by contraction (unpaired *t*-test), which was not observed with compound 4 treatment (Fig. 11*G*). A significant drop in AEC was observed only in contracting EDL from NT5C1A-knockout mice (Fig. 11*C*). The rise in IMP induced by electrical stimulation of EDL from wild-type mice was significantly ablated by ~50% in muscles preincubated with compound 4, which is similar to the effect of the compound in contracting rat epitrochlearis muscle (19) and

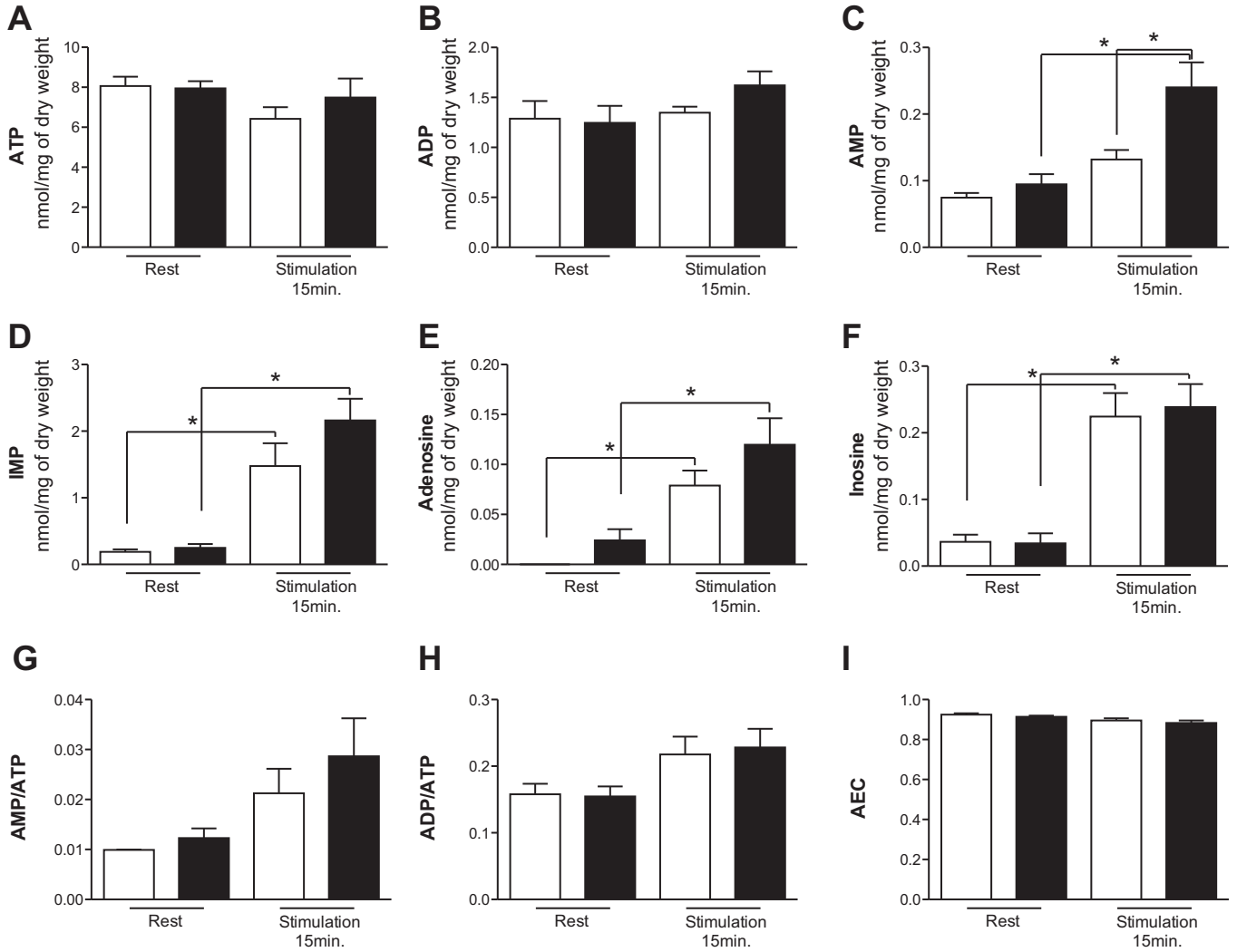

Fig. 7. Purine nucleotide levels in soleus muscles from wild-type vs. NT5C2-knockout mice incubated with and without electrical stimulation. Soleus muscles from wild-type (open bars) and NT5C2-knockout (black bars) mice were incubated without electrical stimulation (Rest) or subjected to electrical stimulation for 15 min as described in MATERIALS AND METHODS. Total purine nucleotide concentrations were measured in perchlorate extracts by HPLC and expressed as nmol/mg of muscle dry weight (*A–F*) for calculations of AMP:ATP ratio (*G*), ADP:ATP ratio (*H*), and adenylate energy charge (AEC) (*I*). Values are means ± SE of five separate experiments and the data were analyzed by one-way ANOVA. *Significant difference, $P < 0.05$.

indicates that compound treatment was effectively inhibiting AMPD1 (Fig. 11*D*). The effect of compound treatment to decrease IMP was lost in muscles from NT5C1A-knockout mice, possibly because of the block in AMP hydrolysis and incomplete inhibition of AMPD1 by compound 4 (Fig. 11*D*). In EDL from wild-type mice, the contraction-induced increase in adenosine levels was enhanced threefold by treatment with compound 4, consistent with AMPD1 inhibition, and this increase was abrogated by NT5C1A deletion (Fig. 11*E*). The increase in inosine levels observed in electrically stimulated EDL from wild-type mice was unaffected by treatment with compound 4, again possibly due to incomplete AMPD1 inhibition, and the increase in inosine levels was abrogated in contracting EDL from NT5C1A-knockout mice treated with or without the AMPD inhibitor compound 4 (Fig. 11*F*). A similar slight decrease in AEC was significant only in contracting EDL from NT5C1A-knockout mice either treated with or not treated with compound 4 (Fig. 11*I*).

AMPK activation observed after electrical stimulation of EDL from wild-type mice was not enhanced in muscles that had been preincubated with the AMPD inhibitor compound 4 (Fig. 12, *A–C*). This contrasts with our previous results in rat epitrochlearis muscle in which compound 4 treatment potentiated AMPK Thr^{172} and downstream ACC phosphorylation, and which is observed during contraction (19). Furthermore, in EDL from NT5C1A-knockout mice, there was no enhancement of AMPK activation by contraction either with or without treatment with compound 4 (Fig. 12*A*). Also, similar increases in AMPKα $pThr^{172}$ and ACC $pSer^{212}$ phosphorylation observed in electrically stimulated EDL from wild-type vs. NT5C1A-knockout mice were unaffected by preincubating muscles with compound 4 (Fig. 12, *B* and C). Interestingly, contraction led to similar increases in AMPKα_1/α_2 $Ser^{485/491}$ phosphorylation in EDL from wild-type and NT5C1A-knockout mice (Fig. 12, *B* and *C*), which was perhaps higher in muscles preincubated with compound 4 (Fig. 12*C*). Finally,

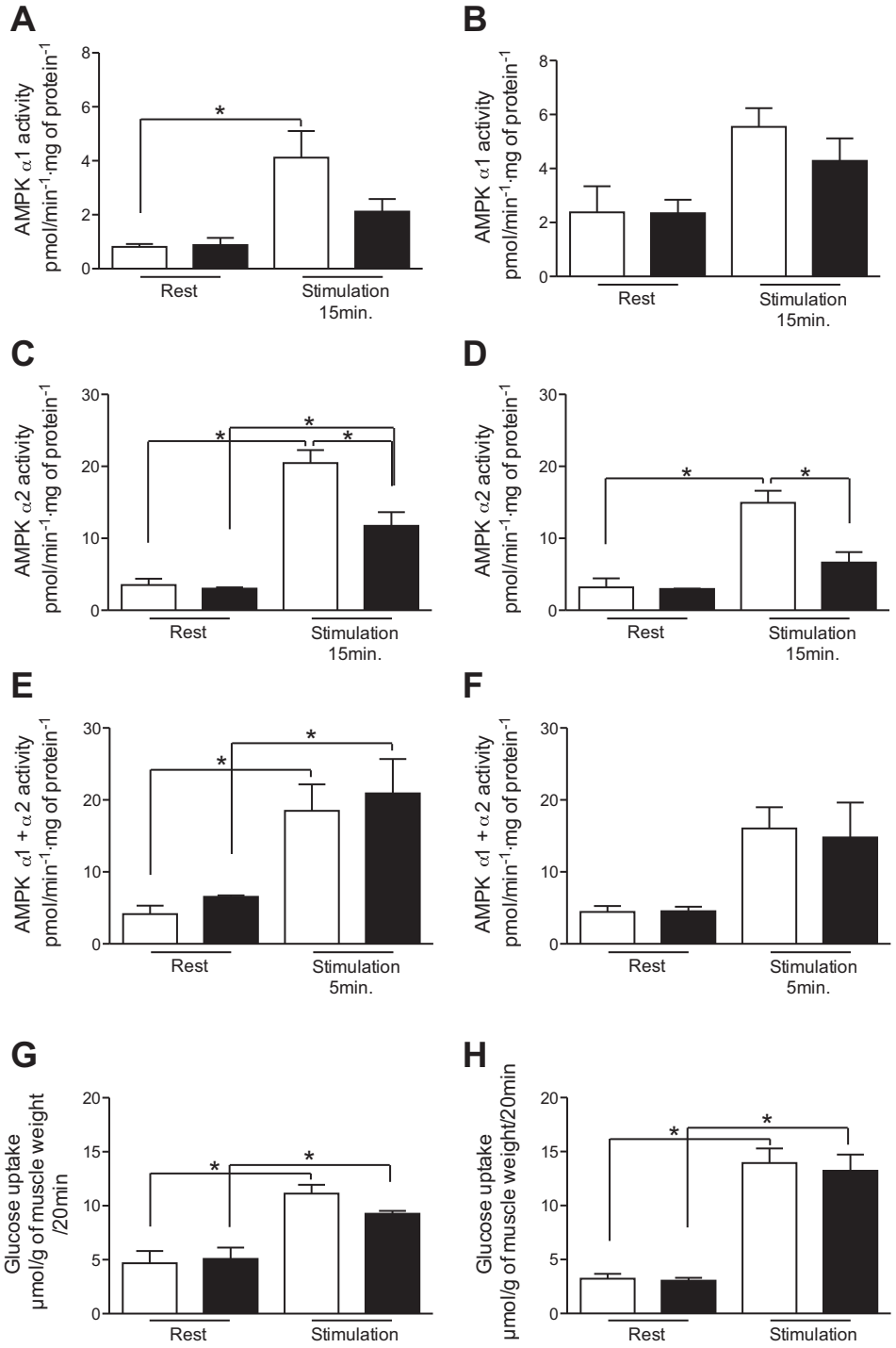

Fig. 8. AMPK activities and glucose uptake in skeletal muscles from wild-type vs. NT5C1A-knockout mice incubated with and without electrical stimulation. EDL (*A* and *C*) and soleus (*B* and *D*) muscles from wild-type (open bars) vs. NT5C1A-knockout (black bars) mice were incubated without electrical stimulation (Rest) or subjected to electrical stimulation for 15 min. Extracts were immunoprecipitated with anti-AMPKα_1 (*A* and *B*) or anti-AMPKα_2 (*C* and *D*) antibodies before AMPK assay. Values are means ± SE of three separate experiments. EDL (*E*) and soleus (*F*) muscles were also incubated with or without electrical stimulation for 5 min and extracts were immunoprecipitated with anti-AMPKα_1 plus anti-AMPKα_2 antibodies before AMPK assay. Values are means ± SE of three separate experiments. Glucose uptake was measured in electrically stimulated or resting muscles as described in the legend for Fig. 5. Values are means ± SE of four separate experiments and the data were analyzed by one-way ANOVA. *Significant difference, $P < 0.05$.

NT5C1A deletion did not appear to cause large changes in expression levels in EDL of the major AMPK subunits found in skeletal muscle (except perhaps for AMPKγ_3, the expression of which seemed lower in wild-type EDL) (Fig. 12*D*). Thus, there was no decrease in AMPK subunit expression in NT5C1A-knockout EDL that could explain reduced AMPK activation by contraction (Fig. 8*C*). Taken together, the findings show that dual targeting of NT5C1A and AMPD1 did not result in enhanced AMPK activation in response to contraction in mouse EDL muscle.

DISCUSSION

In the present study, we further investigated whether inhibition of AMP-metabolizing enzymes could be exploited as a strategy to enhance AMPK activation and glucose uptake in skeletal muscle for the treatment of T2D. NT5C1A- and NT5C2-knockout mice were generated displaying no obvious phenotype (data not shown). Genetic deletion of NT5C1A and NT5C2 was confirmed by RT-PCR (Figs. 3 and 4). Moreover, deletion of NT5C2 was reflected by a significant increase in

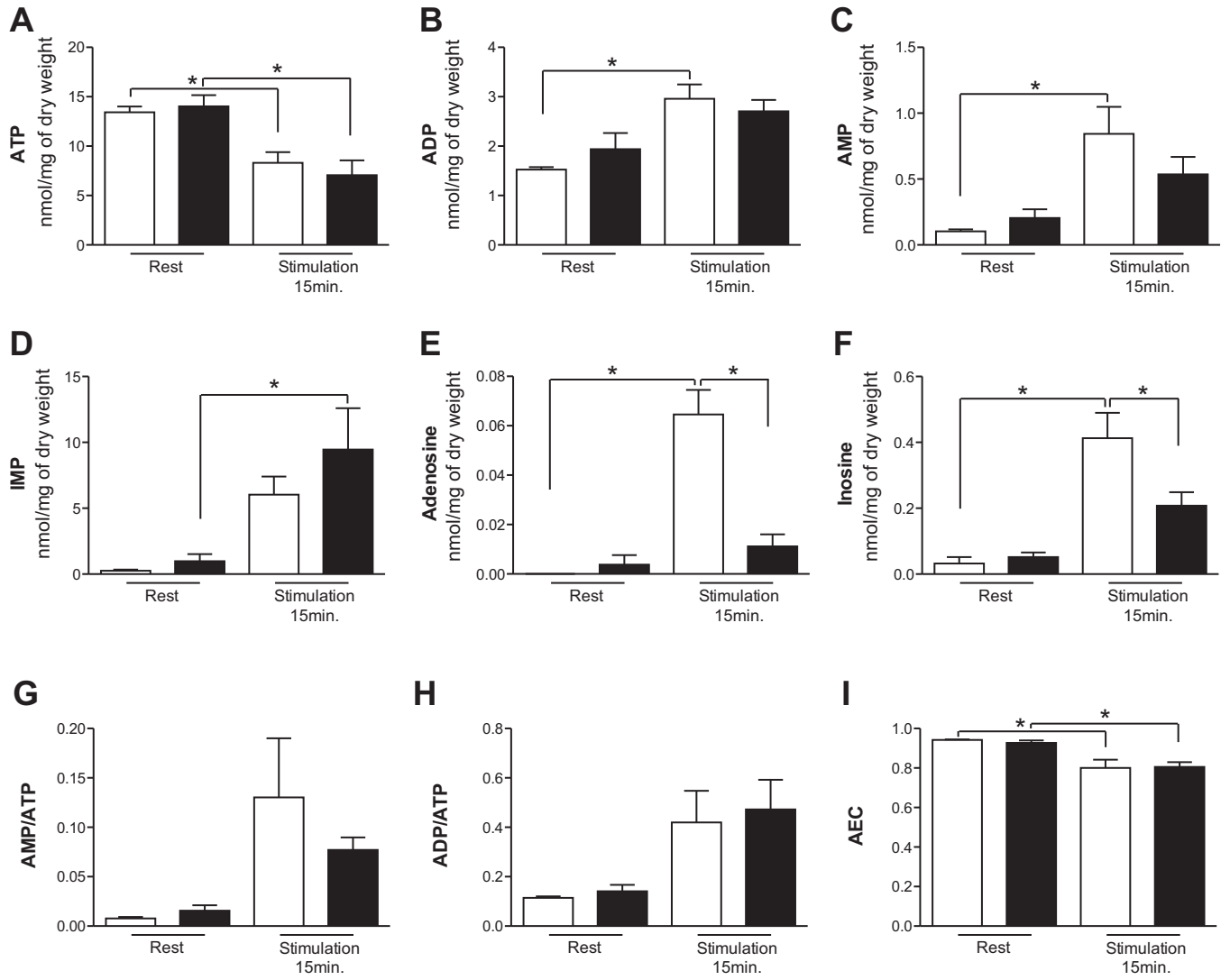

Fig. 9. Purine nucleotide levels in EDL muscles from wild-type vs. NT5C1A-knockout mice incubated with and without electrical stimulation. EDL muscles from wild-type (open bars) and NT5C1A-knockout (black bars) mice were incubated without electrical stimulation (Rest) or subjected to electrical stimulation for 15 min as described in MATERIALS AND METHODS. Total purine nucleotide concentrations were measured in perchlorate extracts by HPLC and expressed as nmol/mg of muscle dry weight (*A–F*) for calculations of AMP:ATP ratio (*G*), ADP:ATP ratio (*H*), and AEC (*I*). Values are means ± SE of five separate experiments and the data were analyzed by one-way ANOVA. *Significant difference, $P < 0.05$.

IMP in EDL following electrical stimulation (Fig. 6*D*), although a rise in inosine during contraction was still observed (Fig. 6*F*), possibly indicating rerouting of AMP through NT5C1A and adenosine deaminase to inosine (Fig. 1). Deletion of NT5C1A was consistent with the marked reduction in the contraction-induced increase in adenosine levels observed in EDL (Fig. 9*E*) and soleus (Fig. 10*E*). Interestingly, the rise in inosine observed after electrical stimulation in EDL from wild-type mice was also significantly decreased in EDL from NT5C1A-knockout mice (Fig. 9*F* and Fig. 11*F*), possibly due to routing of IMP through the salvage pathway via adenylosuccinate to AMP due to NT5C1A deletion.

Our overexpression studies in HEK293 cells indicated that NT5C1A exerted a large proportion of control over AMP and would be a promising drug target for achieving AMPK activation (19). Also, gene silencing of NT5C1A by short hairpin RNA (shRNA) injection and electroporation in mouse TA muscle significantly increased the basal AMP:ATP ratio, increased basal AMPKα Thr^{172} (60%) and downstream ACC phosphorylation (50%), and increased basal glucose uptake, albeit modestly (20%) (11). Also, small interfering RNA (siRNA) silencing of NT5C2 in cultured human myocytes resulted in a twofold increase in basal AMP:ATP ratio, increased AMPKα Thr^{172} phosphorylation 2.4-fold, and slightly increased basal glucose uptake (11). Our findings on genetic deletion of the NT5Cs in muscle are quite unexpected and at variance with these studies. We did not observe significant increases in AMP:ATP ratio in resting EDL or soleus deleted for NT5C1A (Fig. 9*G* and Fig. 10*G*) or for NT5C2 (Fig. 6*G* and Fig. 7*G*), respectively. Moreover, there was no significant potentiation of the increases in AMP:ATP and ADP:ATP ratios as a result of electrical stimulation due to NT5C2 deletion in EDL (Fig. 6, *G* and *H*) and soleus (Fig. 7, *G* and *H*) or NT5C1A deletion in EDL (Fig. 9, *G* and *H*) and soleus (Fig. 10, *G* and *H*).

Total AMPK activities at rest or following 15 min of electrical stimulation were the same in muscles from wild-type

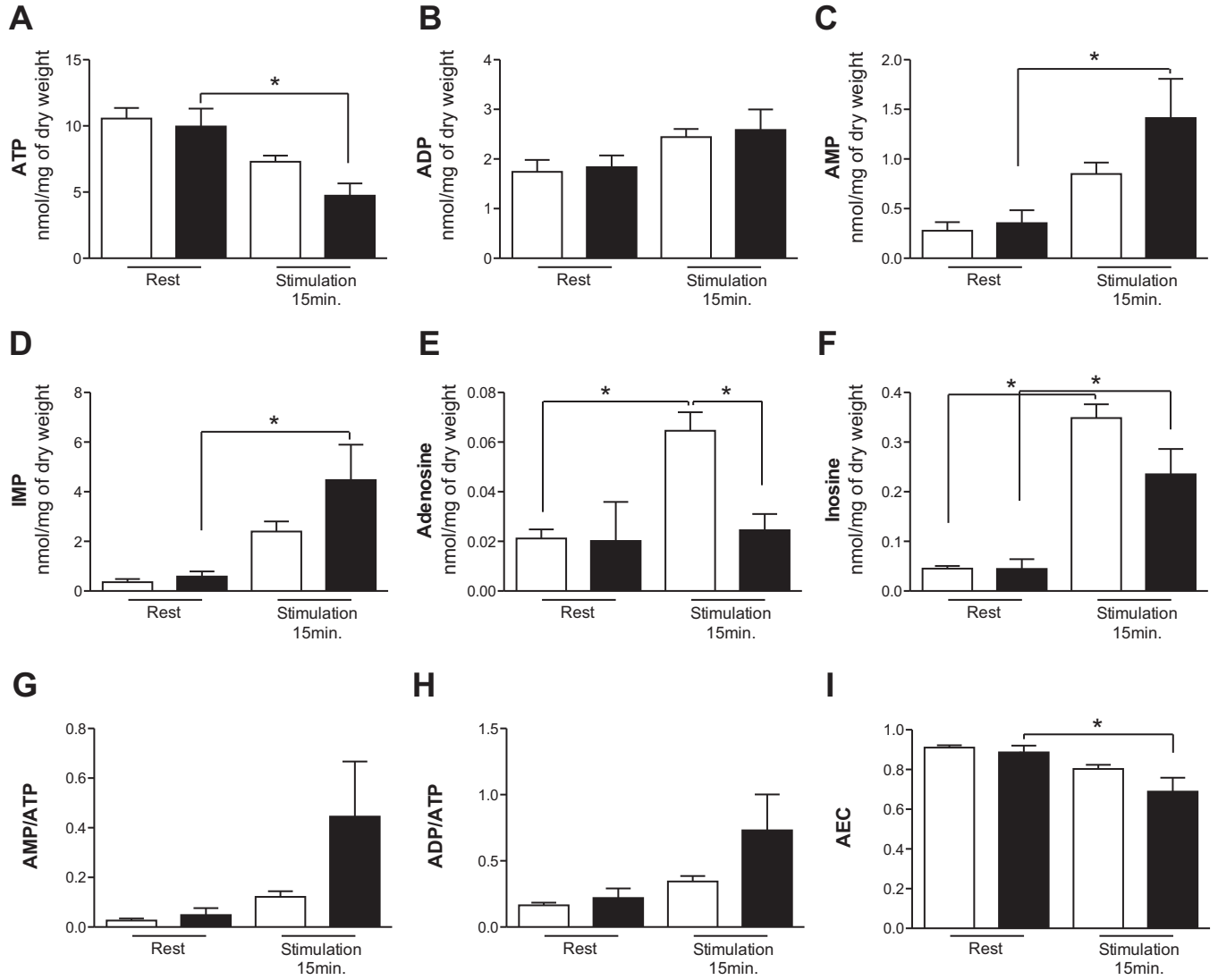

Fig. 10. Purine nucleotide levels in soleus muscles from wild-type vs. NT5C1A-knockout mice incubated with and without electrical stimulation. Soleus muscles from wild-type (open bars) and NT5C1A-knockout (black bars) mice were incubated without electrical stimulation (Rest) or subjected to electrical stimulation for 15 min as described in MATERIALS AND METHODS. Total purine nucleotide concentrations were measured in perchlorate extracts by HPLC and expressed as nmol/mg of muscle dry weight (*A–F*) for calculations of AMP:ATP ratio (*G*), ADP:ATP ratio (*H*), and AEC (*I*). Values are means ± SE of five separate experiments and the data were analyzed by one-way ANOVA. *Significant difference, $P < 0.05$.

and NT5C2 knockout mice (Fig. 5, *A* and *B*). AMPK activities of AMPKα_1- and AMPKα_2-containing complexes were the same in EDL and soleus from NT5C1A-knockout vs. wild-type mice at rest (Fig. 8, *A–D*). NT5C1A deletion resulted in significantly reduced AMPKα_2 activation in EDL (Fig. 8*C*) and soleus (Fig. 8*D*) after 15 min of electrical stimulation, even though there were no significant differences in the increases in AMP levels or AMP:ATP ratios induced by contraction in EDL (Fig. 9, *C* and *G*) or soleus (Fig. 10, *C* and *G*) muscles from wild-type vs. NT5C1A-knockout mice. Also, downstream ACC phosphorylation appeared to increase to the same extent in EDL from wild-type and NT5C1A-knockout mice following electrical stimulation (Fig. 12, *B* and *C*), and after 5 min of electrical stimulation of EDL and soleus from NT5C1A-knockout vs. wild-type mice, AMPK activation of AMPKα_1- plus AMPKα_2-containing complexes was the same (Fig. 8, *E* and *F*). We previously demonstrated that AMPKα_1/α_2 Ser$^{485/491}$ phosphorylation by insulin in perfused rat hearts inhibited AMPKα Thr^{172} phosphorylation/AMPK activation in a subsequent ischemic episode (9). Interestingly, increased inhibitory AMPKα_1/α_2 Ser^{485}/Ser^{491} phosphorylation was observed in EDL after 15 min of electrical stimulation, but the increase appeared to be the same in muscles from wild-type and NT5C1A-knockout mice and seemed to increase further on preincubation with compound 4 (Fig. 12, *B* and *C*). Thus, increased AMPKα_1/α_2 Ser^{485}/Ser^{491} phosphorylation would probably not explain the decrease in AMPKα_2 activation in NT5C1A EDL observed after 15 min of electrical stimulation (Fig. 8*C*) and we have no explanation why total AMPK activation in NT5C1A EDL and soleus was not reduced in muscles contracted for 5 min (Fig. 8, *E* and *F*). Contraction-induced increases in glucose uptake in EDL and soleus from wild-type vs. NT5C1A-knockout mice were similar (Fig. 8, *E* and

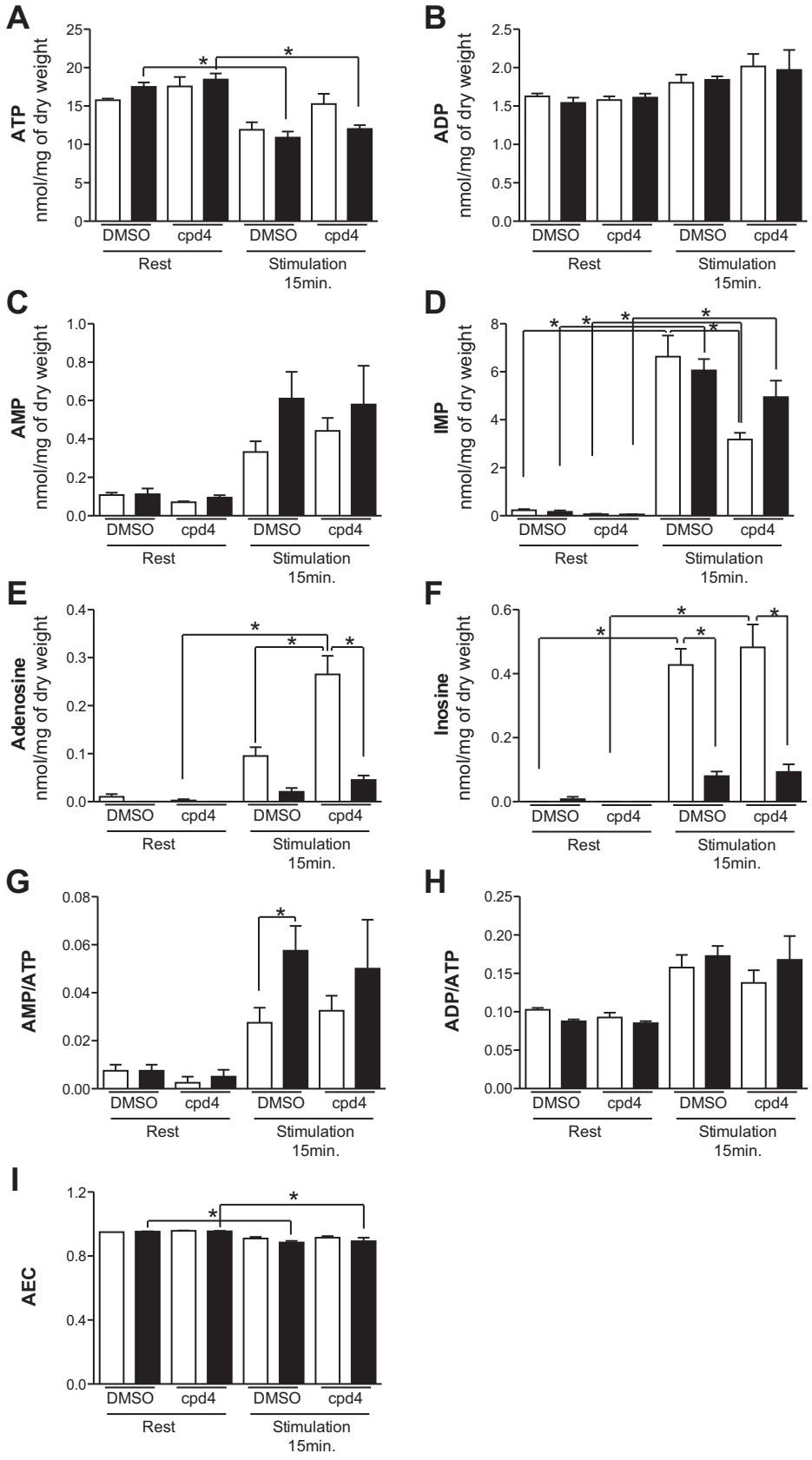

Fig. 11. Purine nucleotide levels in EDL muscles from wild-type vs. NT5C1A-knockout mice preincubated with or without AMPD inhibitor compound 4 and incubated with and without electrical stimulation. EDL from wild-type (open bars) and NT5C1A-knockout (black bars) mice were preincubated with DMSO or AMPD inhibitor compound 4 (cpd4) for 60 min and incubated without electrical stimulation (Rest) or subjected to electrical stimulation for 15 min as described in MATERIALS AND METHODS. Total purine nucleotide concentrations were measured in perchlorate extracts by HPLC and expressed as nmol/mg of muscle dry weight (*A–F*) for calculations of AMP:ATP ratio (*G*), ADP:ATP ratio (*H*), and AEC (*I*). Values are means ± SE of four separate experiments and the data were analyzed by two-way ANOVA and by unpaired *t*-test (*G*). *Significant difference, $P < 0.05$.

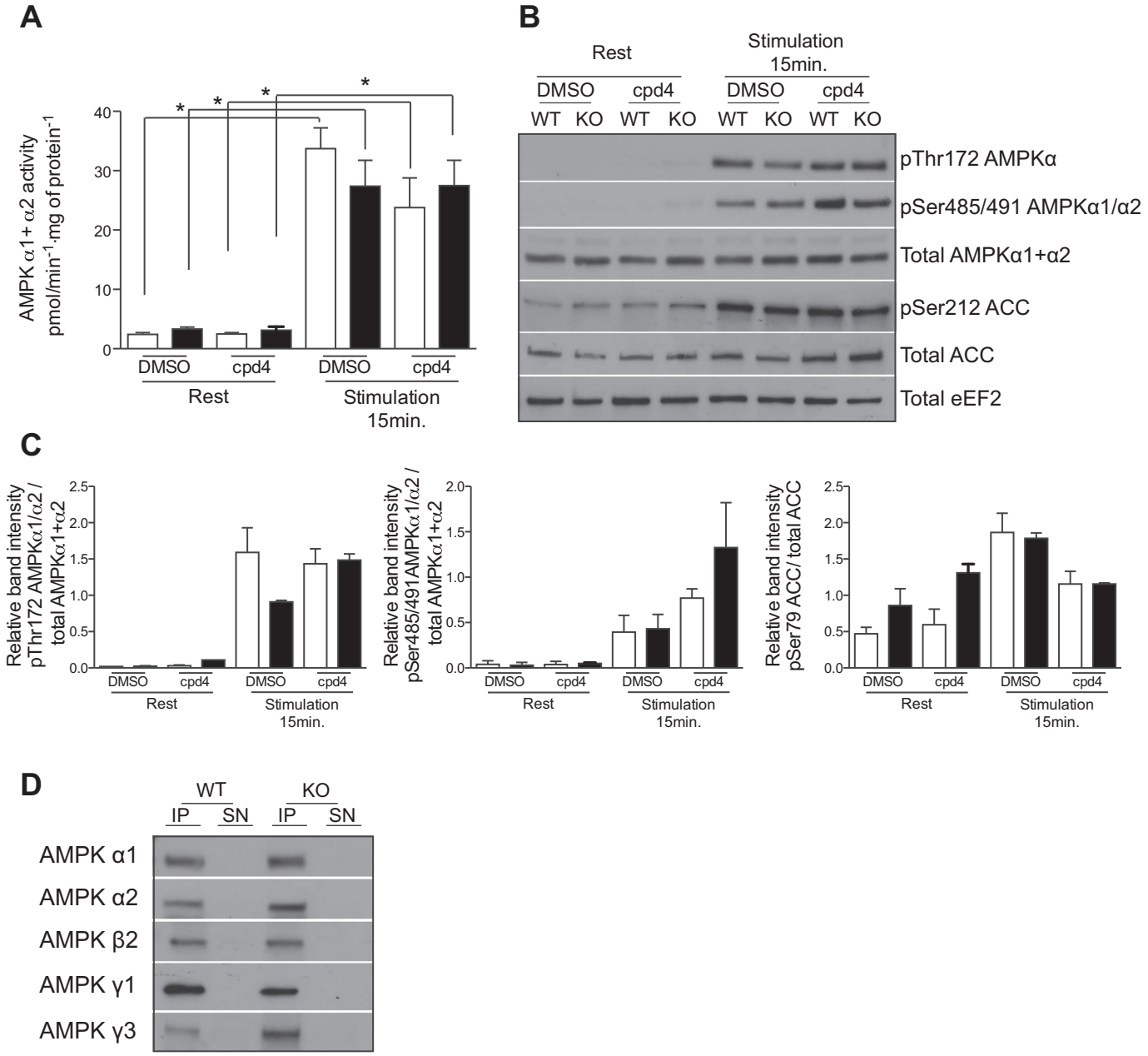

Fig. 12. AMPK activities, and AMPK and ACC phosphorylation in EDL muscles from wild-type vs. NT5C1A-knockout mice preincubated with or without AMPD inhibitor compound 4 (cpd4) and incubated with and without electrical stimulation together with AMPK subunit expression levels. *A*: EDL from wild-type (open bars) and NT5C1A-knockout (black bars) mice were preincubated with DMSO or AMPD inhibitor cpd4 for 60 min and incubated without electrical stimulation (Rest) or subjected to electrical stimulation for 15 min as described in MATERIALS AND METHODS. *A*: extracts were immunoprecipitated with anti-AMPKα_1 plus anti-AMPKα_2 antibodies for AMPK assay. Values are means ± SE of three (Rest) and four (Stimulation) separate experiments and the data were analyzed by one-way ANOVA. *Significant difference, $P < 0.05$. *B*: EDL extracts were immunoblotted with the indicated antibodies and a representative blot is shown. *C*: signals obtained with anti-pThr^{172} AMPK, anti-pSer$^{485/491}$ AMPKα_1/α_2, and anti-p212ACC antibodies were quantified by scanning densitometry and expressed relative to band intensities obtained with anti-total AMPKα_1 + α_2 antibodies or anti-total ACC (means ± range of two separate experiments). *D*: extracts were prepared from EDL incubated at rest for immunoprecipitation with anti-AMPKβ_1 plus anti-AMPKβ_2 antibodies as described in MATERIALS AND METHODS followed by immunoblotting the immunoprecipitate (IP) and supernatant (SN) with the indicated antibodies. A representative blot of two separate experiments is shown.

F) and unaffected by reduced AMPKα_2 activation observed in muscles from NT5C1A-knockout mice that were electrically stimulated for 15 min (Fig. 8, *C* and *D*).

One could argue that there was a tendency toward increased AMP levels in contracting EDL (Fig. 6*C*) and soleus (Fig. 7*C*) from NT5C2-knockout mice together with a trend toward an increased AMP:ATP ratio in NT5C2-knockout soleus (Fig. 7*G*). Also, there was a tendency toward increased AMP in electrically stimulated NT5C1A-knockout soleus (Fig. 10*C*) as well as a trend toward an increase in AMP:ATP ratio (Fig. 10*G*) and the AEC was significantly lower in contracting NT5C1A-knockout soleus (Fig. 10*I*). Although it may appear that there was a trend toward enhanced AMP levels (Fig. 10*C*) and AMP:ATP ratio (Fig. 10*G*) by contraction due to NT5C1A

deletion in soleus, inspection of the individual values revealed that this was not the case. In the set of experiments on contracting EDL from NT5C1A-knockout vs. wild-type mice there was a tendency toward increased AMP concentrations (Fig. 11*C*), but the increase was not significant either by ANOVA or by unpaired *t*-test. The rise in AMP:ATP ratio (Fig. 11*G*) in contracting EDL from NT5C1A-knockout vs. wild-type mice was not significant by ANOVA but was significant by unpaired *t*-test. In the other set of experiments on EDL from NT5C1A-knockout vs. wild-type mice, there was clearly no effect of electrical stimulation on AMP concentrations (Fig. 9*C*) or on AMP:ATP ratio (Fig. 9*G*). The only difference between the two sets of experiments was a 60-min preincubation with DMSO (Fig. 11) before electrical stimulation because some muscles were treated with compound 4 in parallel. Thus, although NT5C1A deletion in EDL may increase the AMP:ATP ratio in the set of experiments shown in Fig. 11, this increase did not translate into enhanced contraction-induced AMPK activation (Fig. 12). Because an increase in AMP concentration would allosterically stimulate AMPK and cause stable AMPK activation via increased AMPKα Thr^{172} phosphorylation, we monitored downstream ACC phosphorylation to detect increases in AMPK activity due to the allosteric effect. However, the increases in ACC phosphorylation induced by contraction in wild-type vs. NT5C2-knockout EDL and soleus muscles (Fig. 5, *E* and *F*) as well as wild-type vs. NT5C1A-knockout EDL (Fig. 12*B*) were similar. Therefore, we believe that NT5C deletions really do not alter AMP concentrations and that statistical power was sufficient to detect changes in nucleotide levels in our muscle experiments.

Surprisingly, combined blockade of AMP metabolism using AMPD inhibitor compound 4 (19) and NT5C1A deletion did not affect the increased AMP:ATP ratio induced by contraction (Fig. 10*G*) or lead to enhanced AMPK activity, either at rest or after electrical stimulation (Fig. 12). The results on muscles from the NT5C-knockout mice contradict previous findings in which AMP levels and AMPK activity were shown to be modulated by NT5C enzymes (11, 19). Taken together with our previous work on pharmacological AMPD1 inhibition and AMPD1 genetic deletion in muscle (19) and the fact that administration of AMPD inhibitors in insulin-resistant or diabetic rodent disease models did not improve glucose control (1), we conclude that pharmacological inhibition of AMP-metabolizing enzymes would not be a viable strategy for increasing AMPK activity and glucose uptake in muscle for the treatment of T2D. It is possible that the fluxes through NT5C1A and NT5C2 during skeletal muscle contraction are too low to affect AMP levels for pharmacological inhibition to be exploited.

ACKNOWLEDGMENTS

We thank Louis Hue for his advice and interest during this study.

GRANTS

Support for this study was provided by the Interuniversity Poles of Attraction Belgian Science Policy Grants P6/28 and P7/13, by the Directorate General Higher Education and Scientific Research, French Community of Belgium and by Fonds de la Recherche Scientifique (FNRS, Belgium) through Grants 3.4518.11 and T.0008.15. S. Kviklyte was supported by Interuniversity Poles of Attraction Belgian Science Policy Grant P7/13, and D. Vertommen was "Collaborateur Logistique" at FNRS, Belgium, and is now "Logistician de Recherche Principal" (UCL).

DISCLOSURES

No conflicts of interest, financial or otherwise, are declared by the authors.

AUTHOR CONTRIBUTIONS

S.K., P.G., and M.H.R. conceived and designed research; S.K., D.V., X.Y., H.A., and X.X. performed experiments; S.K. and M.H.R. analyzed data; M.H.R. interpreted results of experiments; S.K. and H.A. prepared figures; S.K. and M.H.R. drafted manuscript; M.H.R. edited and revised manuscript; S.K., D.V., X.Y., H.A., X.X., P.G., M.B.-Y., J.O., and M.H.R. approved final version of manuscript.

REFERENCES

1. **Admyre T, Amrot-Fors L, Andersson M, Bauer M, Bjursell M, Drmota T, Hallen S, Hartleib-Geschwindner J, Lindmark B, Liu J, Löfgren L, Rohman M, Selmi N, Wallenius K.** Inhibition of AMP deaminase activity does not improve glucose control in rodent models of insulin resistance or diabetes. *Chem Biol* 21: 1486–1496, 2014. doi:10.1016/j.chembiol.2014.09.011.
2. **Bianchi V, Spychala J.** Mammalian 5′-nucleotidases. *J Biol Chem* 278: 46195–46198, 2003. doi:10.1074/jbc.R300032200.
3. **Bradford MM.** A rapid and sensitive method for the quantitation of microgram quantities of protein utilizing the principle of protein-dye binding. *Anal Biochem* 72: 248–254, 1976. doi:10.1016/0003-2697(76)90527-3.
4. **Bultot L, Jensen TE, Lai YC, Madsen AL, Collodet C, Kviklyte S, Deak M, Yavari A, Foretz M, Ghaffari S, Bellahcene M, Ashrafian H, Rider MH, Richter EA, Sakamoto K.** Benzimidazole derivative small-molecule 991 enhances AMPK activity and glucose uptake induced by AICAR or contraction in skeletal muscle. *Am J Physiol Endocrinol Metab* 311: E706–E719, 2016. doi:10.1152/ajpendo.00237.2016.
5. **Cool B, Zinker B, Chiou W, Kifle L, Cao N, Perham M, Dickinson R, Adler A, Gagne G, Iyengar R, Zhao G, Marsh K, Kym P, Jung P, Camp HS, Frevert E.** Identification and characterization of a small molecule AMPK activator that treats key components of type 2 diabetes and the metabolic syndrome. *Cell Metab* 3: 403–416, 2006. doi:10.1016/j.cmet.2006.05.005.
6. **DeFronzo RA.** Lilly lecture 1987. The triumvirate: beta-cell, muscle, liver. A collusion responsible for NIDDM. *Diabetes* 37: 667–687, 1988. doi:10.2337/diab.37.6.667.
7. **Foretz M, Guigas B, Bertrand L, Pollak M, Viollet B.** Metformin: from mechanisms of action to therapies. *Cell Metab* 20: 953–966, 2014. doi:10.1016/j.cmet.2014.09.018.
8. **Hardie DG.** AMPK—sensing energy while talking to other signaling pathways. *Cell Metab* 20: 939–952, 2014. doi:10.1016/j.cmet.2014.09.013.
9. **Horman S, Vertommen D, Heath R, Neumann D, Mouton V, Woods A, Schlattner U, Wallimann T, Carling D, Hue L, Rider MH.** Insulin antagonizes ischemia-induced Thr^{172} phosphorylation of AMP-activated protein kinase α-subunits in heart via hierarchical phosphorylation of $Ser^{485/491}$. *J Biol Chem* 281: 5335–5340, 2006. doi:10.1074/jbc.M506850200.
10. **Hunsucker SA, Spychala J, Mitchell BS.** Human cytosolic 5′-nucleotidase I: characterization and role in nucleoside analog resistance. *J Biol Chem* 276: 10498–10504, 2001. doi:10.1074/jbc.M011218200.
11. **Kulkarni SS, Karlsson HK, Szekeres F, Chibalin AV, Krook A, Zierath JR.** Suppression of 5′-nucleotidase enzymes promotes AMP-activated protein kinase (AMPK) phosphorylation and metabolism in human and mouse skeletal muscle. *J Biol Chem* 286: 34567–34574, 2011. doi:10.1074/jbc.M111.268292.
12. **Lai YC, Kviklyte S, Vertommen D, Lantier L, Foretz M, Viollet B, Hallén S, Rider MH.** A small-molecule benzimidazole derivative that potently activates AMPK to increase glucose transport in skeletal muscle: comparison with effects of contraction and other AMPK activators. *Biochem J* 460: 363–375, 2014. doi:10.1042/BJ20131673.
13. **Lai YC, Zarrinpashneh E, Jensen J.** Additive effect of contraction and insulin on glucose uptake and glycogen synthase in muscle with different glycogen contents. *J Appl Physiol (1985)* 108: 1106–1115, 2010. doi:10.1152/japplphysiol.00401.2009.
14. **Langendorf CG, Kemp BE.** Choreography of AMPK activation. *Cell Res* 25: 5–6, 2015. doi:10.1038/cr.2014.163.
15. **Liu Y, Lai YC, Hill EV, Tyteca D, Carpentier S, Ingvaldsen A, Vertommen D, Lantier L, Foretz M, Dequiedt F, Courtoy PJ, Erneux C, Viollet B, Shepherd PR, Tavaré JM, Jensen J, Rider MH.** Phosphatidylinositol 3-phosphate 5-kinase (PIKfyve) is an AMPK target par-

ticipating in contraction-stimulated glucose uptake in skeletal muscle. *Biochem J* 455: 195–206, 2013. doi:10.1042/BJ20130644.

16. **Mahnke-Zizelman DK, Tullson PC, Sabina RL.** Novel aspects of tetramer assembly and N-terminal domain structure and function are revealed by recombinant expression of human AMP deaminase isoforms. *J Biol Chem* 273: 35118–35125, 1998. doi:10.1074/jbc.273.52.35118.
17. **Morisaki T, Sabina RL, Holmes EW.** Adenylate deaminase. A multigene family in humans and rats. *J Biol Chem* 265: 11482–11486, 1990.
18. **Ogasawara N, Goto H, Yamada Y, Watanabe T.** Distribution of AMP-deaminase isozymes in rat tissues. *Eur J Biochem* 87: 297–304, 1978. doi:10.1111/j.1432-1033.1978.tb12378.x.
19. **Plaideau C, Lai YC, Kviklyte S, Zanou N, Löfgren L, Andersén H, Vertommen D, Gailly P, Hue L, Bohlooly-Y M, Hallén S, Rider MH.** Effects of pharmacological AMP deaminase inhibition and *Ampd1* deletion on nucleotide levels and AMPK activation in contracting skeletal muscle. *Chem Biol* 21: 1497–1510, 2014. doi:10.1016/j.chembiol.2014.09.013.
20. **Plaideau C, Liu J, Hartleib-Geschwindner J, Bastin-Coyette L, Bontemps F, Oscarsson J, Hue L, Rider MH.** Overexpression of AMP-metabolizing enzymes controls adenine nucleotide levels and AMPK activation in HEK293T cells. *FASEB J* 26: 2685–2694, 2012. doi:10.1096/fj.11-198168.
21. **Richter EA, Hargreaves M.** Exercise, GLUT4, and skeletal muscle glucose uptake. *Physiol Rev* 93: 993–1017, 2013. doi:10.1152/physrev.00038.2012.
22. **Sakamoto K, Holman GD.** Emerging role for AS160/TBC1D4 and TBC1D1 in the regulation of GLUT4 traffic. *Am J Physiol Endocrinol Metab* 295: E29–E37, 2008. doi:10.1152/ajpendo.90331.2008.
23. **Sala-Newby GB, Skladanowski AC, Newby AC.** The mechanism of adenosine formation in cells. Cloning of cytosolic 5′-nucleotidase-I. *J Biol Chem* 274: 17789–17793, 1999. doi:10.1074/jbc.274.25.17789.
24. **Steinberg GR, Kemp BE.** AMPK in health and disease. *Physiol Rev* 89: 1025–1078, 2009. doi:10.1152/physrev.00011.2008.
25. **Tozzi MG, Pesi R, Allegrini S.** On the physiological role of cytosolic 5′-nucleotidase II (cN-II): pathological and therapeutical implications. *Curr Med Chem* 20: 4285–4291, 2013. doi:10.2174/09298673113203400007.
26. **Xiao B, Heath R, Saiu P, Leiper FC, Leone P, Jing C, Walker PA, Haire L, Eccleston JF, Davis CT, Martin SR, Carling D, Gamblin SJ.** Structural basis for AMP binding to mammalian AMP-activated protein kinase. *Nature* 449: 496–500, 2007. doi:10.1038/nature06161.
27. **Xiao B, Sanders MJ, Carmena D, Bright NJ, Haire LF, Underwood E, Patel BR, Heath RB, Walker PA, Hallen S, Giordanetto F, Martin SR, Carling D, Gamblin SJ.** Structural basis of AMPK regulation by small molecule activators. *Nat Commun* 4: 3017, 2013. doi:10.1038/ncomms4017.
28. **Zanou N, Shapovalov G, Louis M, Tajeddine N, Gallo C, Van Schoor M, Anguish I, Cao ML, Schakman O, Dietrich A, Lebacq J, Ruegg U, Roulet E, Birnbaumer L, Gailly P.** Role of TRPC1 channel in skeletal muscle function. *Am J Physiol Cell Physiol* 298: C149–C162, 2010. doi:10.1152/ajpcell.00241.2009.